Toxicon: X 2 (2019) 100010

Contents lists available at ScienceDirect

Toxicon: X

journal homepage: www.journals.elsevier.com/toxicon-x

Fluorescent analogues of BeKm-1 with high and specific activity against the hERG channel

Lucie Vasseur[a], Alain Chavanieu[a], Stéphanie Combemale[c], Cécile Caumes[c], Rémy Béroud[c], Michel De Waard[c,d], Pierre Ducrot[b], Jean A. Boutin[b], Gilles Ferry[b], Thierry Cens[a,*]

[a] Institut des Biomolécules Max Mousseron, Université de Montpellier, Montpellier, France
[b] Pole d'expertise Biotechnologie, Chimie, Biologie, Institut de Recherches Servier, Croissy-sur-Seine, France
[c] Smartox Biotechnology, Saint-Egrève, France
[d] Institut du Thorax, Inserm UMR 1087/CNRS UMR 6291, LabEx « Ion Channels, Science & Therapeutics », Nantes, France

ARTICLE INFO

Keywords:
hERG
BeKm-1
In silico docking
Electrophysiology
Xenopus laevis oocytes

ABSTRACT

Peptidic toxins that target specifically mammalian channels and receptors can be found in the venom of animals. These toxins are rarely used directly as tools for biochemical experiments, and need to be modified via the attachment of chemical groups (e.g., radioactive or fluorescent moieties). Ideally, such modifications should maintain the toxin specificity and affinity for its target. With the goal of obtaining fluorescent derivatives of BeKm-1, a toxin from the scorpion species *Buthus eupeus* that selectively inhibits the voltage-gated potassium ion channel hERG, we produced four active analogues using a model of BeKm-1 docking to the outer mouth of the channel. In these BeKm-1 analogues, the natural peptide was linked to the fluorescent cyanine 5 (Cy5) probe via four different linkers at Arg^{1} or Arg/Lys^{27}. All analogues retained their specificity towards the hERG channel in electrophysiological experiments but displayed a lesser affinity. These results validate our strategy for designing toxin analogues and demonstrate that different chemical groups can be attached to different residues of BeKm-1.

1. Introduction

Peptide toxins from terrestrial or marine animals represent invaluable tools for studying ion channels in physiological and pathological conditions. In a recent review, Housley et al. established a comprehensive inventory of the effects of the 320 peptide toxins that are found in scorpion venom and that act on 41 different ion channels (Housley et al., 2017). Nevertheless, the repertoire of potentially interesting peptide toxins is far from being fully explored, even in scorpion venom (Bergeron and Bingham, 2012). Occasionally, a single peptide can be detected in the venom of several different species (kurtoxin, which targets voltage-gated Ca^{2+} channels, is found in the venom of *Parabuthus transvaalicus* and *Parabuthus granulatus*), but a considerable number of peptides (~100,000) remains to be investigated. Peptide toxins and their derivatives also represent attractive pharmacological tools or drug leads (de Souza et al., 2018). For instance, dalazatide (ShK-186), a derivative of the ShK toxin isolated from the venom of the sea anemone *Stichodactyla helianthus*, is the first $K_v1.3$ voltage-gated K^+ channel inhibitor used in clinical trials to treat plaque psoriasis (Tarcha et al., 2017). The peptide could also be efficacious in treating multiple sclerosis and rheumatoid arthritis (Beeton et al., 2006; for review Chandy and Norton, 2017).

The crystal structures of the target channels and the precise binding mode of the toxins provide invaluable frameworks to design toxin analogues. Thanks to tremendous progress of single-particle cryo-electron microscopy (Boutin et al., 2016), the structure of an increasingly higher number of membrane proteins is now available. Recently, the structures of the mammalian $K_v10.1$ (EAG-1) and $K_v11.1$ (ERG1, referred herein as hERG) channels have been resolved (Wang and MacKinnon, 2017; Whicher and MacKinnon, 2016). Both channels belong to the eag (ether-a-go-go) family of voltage-gated K^+ channels that are characterized by two intracellular domains, an N-terminal Per-ARNT-Sim (PAS) domain, and a C-terminal cyclic nucleotide-binding homology domain (CNBHD) (Vandenberg et al., 2012). Like the other voltage-gated K^+ channels, hERG is a homotetramer and each subunit contains six transmembrane segments (S1–S6). Segments S1–S4 contribute to the voltage sensor domain (VSD), whereas segments S5–S6 and the loop linking them contribute to the pore domain and ensure the selectivity towards K^+ ions. Various mutations in KCNH2, the gene encoding the hERG channel, cause the long QT syndrome (LQT), a disorder characterized by prolongation of ventricular repolarization that can lead to sudden cardiac death. LQT can also be caused by

* Corresponding author. IBMM, UMR5247, Bât. CRBM, 1919 Route de Mende, 34293 Montpellier, France.
E-mail address: thierry.cens@inserm.fr (T. Cens).

https://doi.org/10.1016/j.toxcx.2019.100010
Received 30 October 2018; Received in revised form 30 January 2019; Accepted 13 February 2019
Available online 23 February 2019

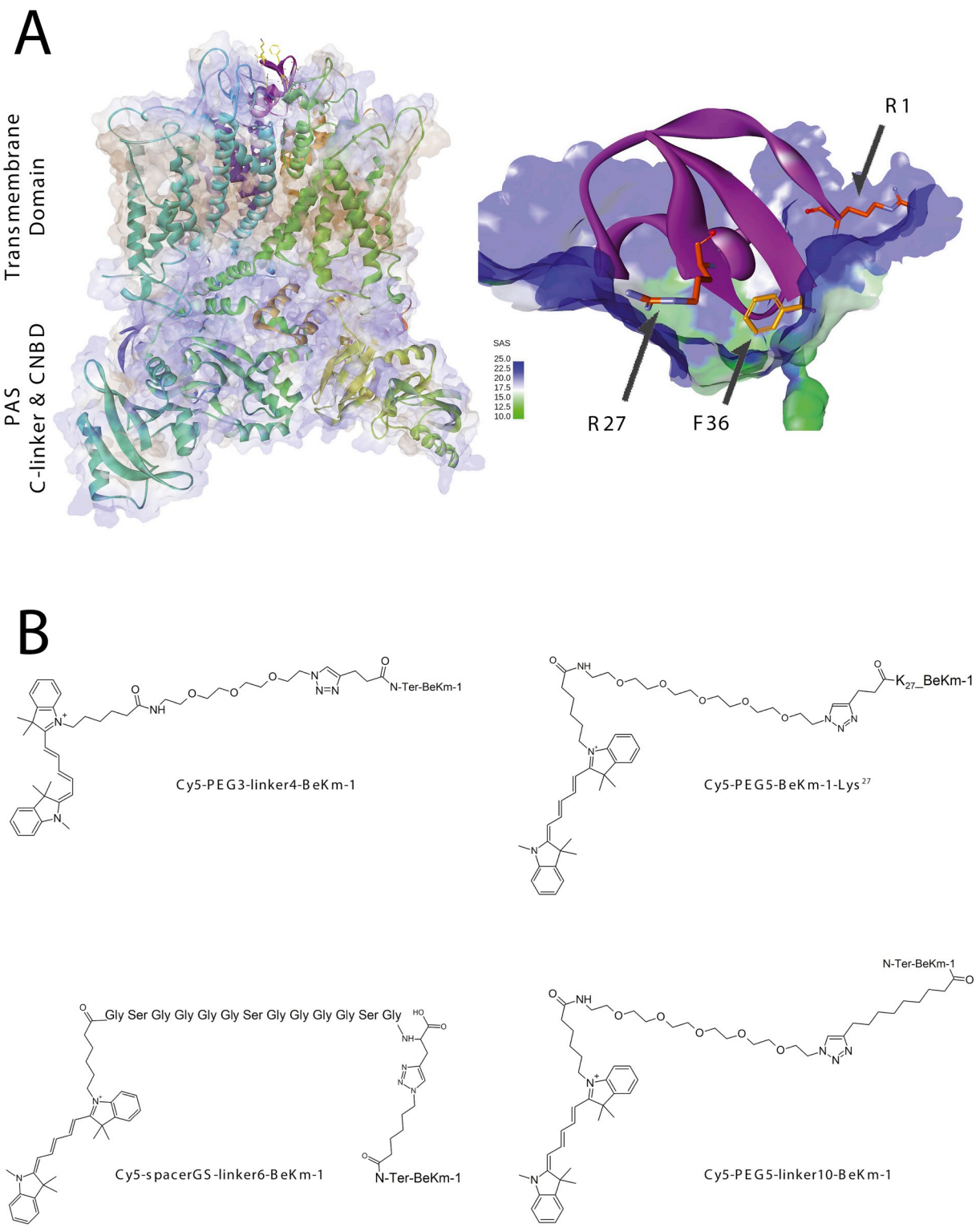

Fig. 1. Docking of BeKm-1 in a model of hERG channel and fluorescent BeKm-1 analogues used in this study. A) Left, BeKm-1 (pdb code: 1j5, magenta, top) in interaction with hERG channel (in solid ribbon representation showing the solvent surface colored by hydrophobicity). The tetrameric model of the hERG channel was generated from the pdb structure (5VA1) using the Prepare Protein module within Discovery Studio. The transmembrane domain, the cytoplasmic N-terminal Per-Arnt-Sim (PAS) domain, the C-terminal C-linker and the cyclic nucleotide binding domain (CNBD) are indicated. Docking of BeKm-1 was performed using the ZDOCK rigid body docking program and refined with the RDOCK module. The top ranked pose of the most populated cluster from the protein-protein interaction predictions is showed with BeKm-1 docked at the top of the transmembrane domain of hERG. Right, Details of the pose of BeKm-1 (magenta) within the interaction surface of hERG colored according to the Solvent Accessibility Surface (SAS) (see Supplementary Data S2), with the side chain of the N terminal Arg^{1} and Arg^{27} (red) and the more buried C terminal Phe^{36} (orange). B) Chemical structures of fluorescent BeKm-1 analogues used in this study with different types of linkers grafted on the N-ter of Arg^{1} or the side chain of Arg^{27} mutated for a Lysine. (For interpretation of the references to color in this figure legend, the reader is referred to the Web version of this article.)

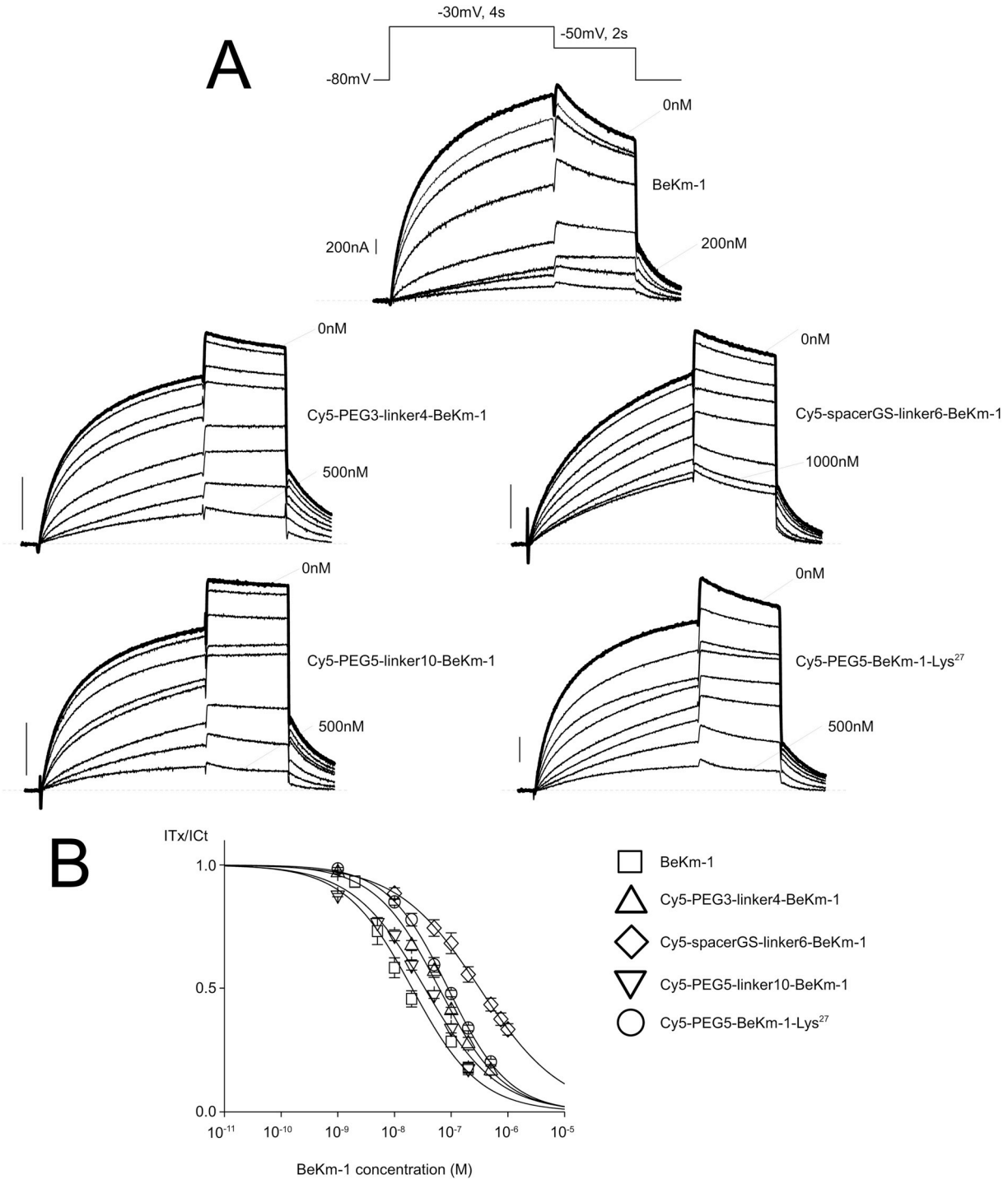

Fig. 2. The fluorescent BeKm-1 analogues potently inhibit hERG currents. A) Typical traces of currents recorded in *Xenopus laevis* oocytes that express hERG. Currents were elicited using the protocol depicted at the top in which a pulse from a holding potential of −80 mV to −30 mV precedes a test pulse at −50 mV, in the presence of increasing concentrations of native BeKm-1, Cy5-PEG3-linker4-BeKm-1, Cy5-spacerGS-linker6-BeKm-1, Cy5-PEG5-linker10-BeKm-1 or Cy5-PEG5-BeKm1-Lys^{27}. Scale bars, 200 nA. B) Inhibition curves of native BeKm-1 and its four analogues. The peak current amplitude was measured during the test pulse at −50 mV in the presence of toxin (ITx) and normalized to the current recorded in the absence of toxin (ICt). Data are the mean ± SEM of n = 4–10 oocytes.

pharmacological agents, such as antibiotics (erythromycin), antipsychotics (chlorpromazine), or antihistamines (terfenadine), that block hERG (Hancox et al., 2008). Interactions with hERG are considered a major obstacle for the development of therapeutic compounds, and for that reason they are studied as early as possible during the discovery process. Beside its role in cardiac physiology hERG expression level is upregulated in various cancer types, suggesting that hERG could be used as a biomarker of cancer invasion (Lastraioli et al., 2015). Despite their structural homology, hERG channels, but not EAG-1 channels, expressed in HEK-293 cells are potently blocked by BeKm-1 (IC_{50} = 3.3 nM), a toxin peptide isolated from the venom of *Buthus eupeus* (Korolkova et al., 2001). Tools to study hERG channels comprise, but are not limited to [^{3}H]dofetilide (Finlayson et al., 2001), [^{3}H]astemizole (Chiu et al., 2004), and [^{125}I]BeKm-1 (Angelo et al., 2003).

In the present work, our aim was to design fluorescent analogues of BeKm-1 that specifically target hERG channels. We established a model

Table 1
Dose-response curve parameters (IC_{50} and hill coefficient (n Hill)) of native BeKm-1 and its four analogues Cy5-PEG3-linker4-BeKm-1, Cy5-spacerGS-linker6-BeKm-1, Cy5-PEG5-linker10-BeKm-1 and Cy5-PEG5-BeKm1-Lys^{27} obtained from *Xenopus laevis* oocytes that express hERG. Data are the mean ± SEM of n oocytes. *p < 0.01 (compared with native BeKm-1).

	BeKm-1 (n = 9)	Cy5-PEG3-linker4-BeKm-1 (n = 6)	Cy5-spacerGS-linker6-BeKm-1 (n = 9)	Cy5-PEG5-linker10-BeKm-1 (n = 9)	Cy5-PEG5-BeKm-1 Lys^{27} (n = 9)
IC_{50} (nM)	12.2 ± 2.2	88.6 ± 7.6 *	280.0 ± 41.8 *	64.1 ± 6.1 *	80.5 ± 10.9 *
n Hill	0.9 ± 0.1	0.8 ± 0.1	0.6 ± 0.1 *	0.8 ± 0.1	0.7 ± 0.1 *

of BeKm-1 docking at the outer mouth of the channel pore using the recently available hERG channel structure. This allowed us to select BeKm-1 residues that are likely to be solvent-exposed and suitable for the attachment of chemical groups without extensively modifying the toxin activity. We then designed four BeKm-1 analogues by grafting a cyanine group on either the N-terminal Arg residue or the Arg^{27} residue mutated to Lys by using different chemical spacers. We evaluated the inhibitory activity of these analogues by electrophysiological recordings in *Xenopus laevis* oocytes that express hERG. All four BeKm-1 analogues retained the toxin inhibitory activity and specificity against the hERG channel and did not affect the human K_v10.1 or K_v1.3 channels. Finally, we demonstrated that BeKm-1 analogues block hERG channels in a manner similar to that of the native toxin. These results validated our strategy for designing toxin analogues and demonstrated that chemical groups can be attached to various residues of the BeKm-1 toxin without altering its specificity and only slightly its affinity for three over four of our analogues.

2. Material and methods

2.1. Modeling BeKm-1 docking to the hERG channel

Based on the hERG channel structure obtained by single-particle cryo-electron microscopy (Protein Data Bank code, 5VA1), the tetrameric hERG channel model was prepared using the 'Prepare Protein' module of Discovery Studio (Dassault System Biovia) where 16 incomplete residues were built and minimized as well as missing residues of the four external loops on each monomer. BeKm-1 binds preferentially to the closed channel conformation of hERG (Milnes et al., 2003); however, only the open conformation was available. We hypothesized that the global organization of the outer transmembrane domain should not be strongly affected by the change from the closed to the open conformation, as previously demonstrated for the KscA potassium channel (Uysal et al., 2009). We also assumed that the global orientation of the bound toxin should not be altered by the gating process. The toxin was docked using the previously established NMR structure of BeKm-1 (Protein Data Bank code, 1J5J). For the initial docking of the entire toxin structure with ZDOCK, no hERG residue was selected as targeted pool and the whole protein surface was made available. The four most populated clusters representing 747 solutions, among a total of 2000 poses, showed a mode of binding to hERG outer mouth with a predominant orientation of the toxin within the binding site. These solutions were refined using the RDOCK program available in Discovery Studio, and the top 100 poses (ranked using the RDock score) were visually analyzed. To select suitable residues for chemical labeling, the solvent accessibility of side chains were observed, mainly to discriminate between the N-terminal and C-terminal residues, as well as to determine the most probable solvent exposed surface of the toxin. The predictive binding mode was compared with a previously modeled complex between BeKm-1 and the hERG channel (Tseng et al., 2007).

2.2. Peptide chemistry and dye coupling to peptides

All peptides [click chemistry-compatible BeKm-1 (3 peptides), BeKm-1 Lys^{27} (1 peptide), and spacer GS (1 peptide)] were assembled stepwise using fmoc solid-phase chemistry on a Symphony Synthesizer (Protein technologies Inc.). Then, 4-pentynoic acid, 6-azido-hexanoic acid, or 10-undecynoic-acid was coupled to the N-terminus of the 36-mer BeKm-1 sequence. In the case of BeKm-1 Lys^{27}, the wild type L-Arg^{27} residue was replaced by L-Lys(pentynoyl)-OH. The spacer GS included L-propargyl glycine (Pra) at the C-terminus with an alkyne function on the side chain, and the Cy5 Acid coupled through a peptide bond at the N-terminus.

All peptides were assembled using a 2-chlorotrityl chloride resin (substitution rate of 1.6 mmol/g). The coupling reaction time for the amino acids was 15 min, and the reaction was repeated twice to increase the amino acid coupling yield. After resin cleavage and deprotection with 92.5% (vol) trifluoroacetic acid, 2.5% H_2O and scavengers (2.5% 1,3-dimethoxybenzene and 2.5% triisopropylsilane), crude toxin analogues were folded/oxidized in 100 mM Tris-HCl, 5 mM GSH/0.5 mM GSSG, pH 8.3 during 24 h. The addition of an alkyne or azide group on Bekm1 did not affect the folding behavior of the toxin. In the case of undecynoic acid, the addition of 1M Guanidinium hydrochloride proved beneficial to limit toxin precipitation. Notably, no concomitant reduction of the azide moiety could be detected during the folding. The resulting oxidized peptides with their three disulfide bridges were purified to homogeneity by C18 reversed phase chromatography (RP-HPLC) on a Jupiter Proteo column (Phenomenex, 4 µm, 21.2 mm ID x 250 mm L) using an Agilent Technologies preparative HPLC system (1260 Infinity). Click chemistry was used to couple Cy5-PEG3-azide to 4-pentynoic-BeKm-1 (final product termed Cy5-PEG3-linker4-BeKm-1); Cy5-PEG5-azide to 10-undecynoic-BeKm-1 (product termed Cy5-PEG5-linker10-BeKm-1); Cy5-spacerGS-Pra to 6-azido-hexanoic-BeKm-1 (product termed Cy5-spacerGS-linker6-BeKm-1); and Cy5-PEG5-azide to BeKm-1 Lys(pentynoyl)-OH (product termed Cy5-PEG5-BeKm-1 Lys^{27}). The peptide-alkyne compound was solubilized by sequential addition of equal volumes of NMP/tBuOH 9:1, distilled water and 0.4 M HEPES containing 50 mM of aminoguanidine to a final peptide concentration of 3 mM. 2 equivalents of the Cy5-azide compound were solubilized in a minimum volume of NMP/tBuOH 9:1 and added to the above peptide solution which was degassed and flushed with Ar. 10 equivalents of Copper(I) bromide dimethylsulfide complex and 50 equivalents of THPTA (Tris-(3-hyroxypropyltriazolylmethyl)amine) were dissolved in a minimum volume of NMP/tBuOH 9:1 and added to the azide-alkyne solution. The pH of the reaction mixture was checked and adjusted to 7–8 if necessary before being degassed and flushed with Ar, then allowed to stir overnight at 40 °C. The reaction was quenched by acidification with formic acid and the mixture was immediately diluted with 6 M Guanidine hydrochloride before purification by RP-HPLC. All products were purified to homogeneity by RP-HPLC, and molecular weights verified by liquid chromatography accurate mass quadrupole time-of-flight mass spectrometry with electrospray ionization (LC-ESI Q-TOF-MS) analysis (Waters Q-TOF Xevo G2S mass spectrometer equipped with an Acquity UHPLC system).

2.3. Molecular biology

Capped cRNA transcripts coding for hERG (NM_000238), hK_v10.1 (NM_172362) and hK_v1.3 (NM_002232) were obtained from linearized plasmids with the mMessage mMachine T7 transcription kit (Thermo-

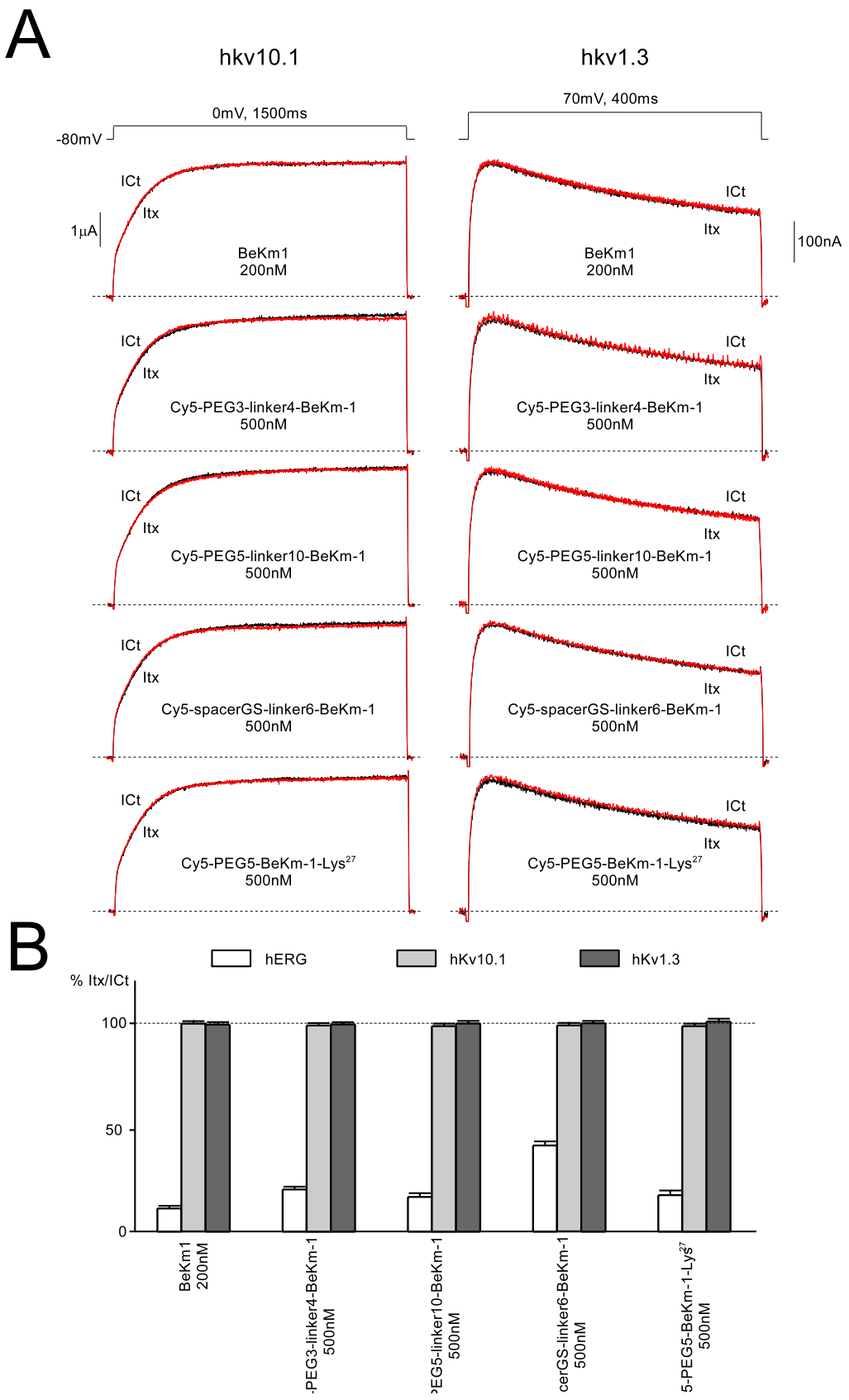

(caption on next page)

Fig. 3. The fluorescent BeKm-1 analogues do not affect hKv10.1 and hKv1.3 currents. A) Typical traces of currents elicited by a step depolarization to 0 mV or 70 mV, from a holding potential of −80 mV, obtained from *Xenopus laevis* oocytes that express hKv10.1 or hKv1.3, respectively, in the absence or presence of 200 nM native BeKm-1 and in the absence or presence of 500 nM of Cy5-PEG3-linker4-BeKm-1, of Cy5-spacerGS-linker6-BeKm-1, of Cy5-PEG5-linker10-BeKm-1 and of Cy5-PEG5-BeKm1-Lys[27]. Note the lack of effect of BeKm-1 and of the four analogues on both channels. B) Percentage of current remaining in the presence of a single dose of native BeKm-1 or its four analogues (Cy5-PEG3-linker4-BeKm-1, Cy5-spacerGS-linker6-BeKm-1, Cy5-PEG5-linker10-BeKm-1 and Cy5-PEG5-BeKm1-Lys[27]). Current amplitude was measured before (ICt) and during (Itx) the perfusion of the different toxins. Data are the mean ± SEM of n = 4–7 oocytes.

Table 2
Percentage of current remaining after exposure to a single dose of native BeKm-1 or its four analogues Cy5-PEG3-linker4-BeKm-1, Cy5-spacerGS-linker6-BeKm-1, Cy5-PEG5-linker10-BeKm-1 and Cy5-PEG5-BeKm1-Lys[27] obtained from *Xenopus laevis* oocytes that express wild type (WT) hERG, $hK_v10.1$ or $hK_v1.3$, or hERG harboring the S631C mutation. Data are the mean ± SEM of n oocytes. *p < 0.01 (compared with WT herg channel).

ITx/ICt (%)	WT hERG	hERG S631C	$hK_v10.1$	$hK_v1.3$
BeKm-1 (200 nM)	11 ± 1% (n = 13)	20 ± 1% * (n = 4)	99 ± 1% * (n = 7)	99 ± 1% * (n = 5)
Cy5-PEG3-linker4-BeKm-1 (500 nM)	20 ± 1% (n = 6)	60 ± 3% * (n = 3)	99 ± 1% * (n = 6)	99 ± 1% * (n = 7)
Cy5-spacerGS-linker6-BeKm-1 (500 nM)	41 ± 2% (n = 9)	87 ± 3% * (n = 4)	99 ± 1% * (n = 6)	99 ± 1% * (n = 7)
Cy5-PEG5-linker10-BeKm-1 (500 nM)	16 ± 2% (n = 9)	40 ± 3% * (n = 3)	99 ± 1% * (n = 6)	99 ± 1% * (n = 7)
Cy5-PEG5-BeKm-1 Lys[27] (500 nM)	17 ± 2% (n = 7)	66 ± 7% * (n = 3)	99 ± 1% * (n = 6)	99 ± 1% * (n = 7)

Fisher) following manufacturer's instructions. The concentrations were adjusted to 1 μg/μL for injection in *Xenopus laevis* oocytes. The S631C mutation in the sequence encoding hERG was introduced by overlap extension PCR. Briefly, hERG cDNA and the primers herg-008S (5′-CATGGCCCGGACGCGCTCCC-3′) and herg-018AS (5′-GAATTCGTGT TGGGGCAGACGTTGCCGAAGC-3′) or herg-019S (5′- CGTCTGCCCCAA CACGAATTCAGAGAAGATC-3′) and herg-004AS (5′- CTAGTGCTGCAG CAGTGAGCGG-3′) were used to PCR amplify two fragments of 1110 bp and 334 bp. The two fragments were purified and subjected to a second round of PCR amplification to obtain a 1423 bp-long fragment that was cloned in pBluescript-SK (Agilent). The presence of the mutation was confirmed by sequencing the entire insert, and then exchanged with the corresponding fragment of the wild-type sequence.

2.4. Electrophysiology

2.4.1. Xenopus laevis oocytes isolation and injection

Stage V–VI oocytes were removed from female *Xenopus laevis* under tricaine anesthesia. Oocytes were defolliculated by incubation with 1 mg/mL collagenase type 1A (Sigma) in OR2 solution (82.5 mM NaCl, 2 mM KCl, 1 mM $MgCl_2$, 5 mM Hepes, pH 7.2 with NaOH) under agitation at room temperature. After intensive washing with OR2 solution, isolated oocytes were maintained at 17 °C in NDS solution (96 mM NaCl, 2 mM KCl, 1.8 mM $CaCl_2$, 1 mM $MgCl_2$, 5 mM Hepes, 2.5 mM sodium-pyruvate, 0.05 mM gentamycin, pH 7.2 with NaOH) renewed daily. RNA solutions (about 30 ng per oocyte) were injected in oocytes on isolation day, and recordings were performed 2–5 days after injection.

2.4.2. Electrophysiological analysis

Expressed currents were recorded at room temperature using the two-electrode voltage clamp method. Electrodes were pulled from borosilicate glass and filled with 3 M KCl. Currents were measured with a Geneclamp 500 amplifier (Molecular Devices), and digitized with a Digidata 1200 converter (Molecular Devices) using the Clampex 5 software (Molecular Devices). Oocytes were clamped at −80 mV and leak currents were subtracted online using a P/3 protocol of hyperpolarizing pre-pulses. Native BeKm-1 (Alomone Labs) and toxin analogues were diluted in the external solution NDherg (96 mM NaCl, 3 mM KCl, 0.5 mM $CaCl_2$, 1 mM $MgCl_2$, 5 mM Hepes, pH 7.4 with NaOH) and perfused through the recording chamber at a rate of 1 mL/min. The concentration to obtain half maximal inhibition (IC_{50}) was determined by measuring the peak tail current recorded during a test pulse at −50 mV in the presence of increasing concentrations of toxin (ITx), and by normalizing the value to the current measured in the absence of toxin (ICt). Data were fitted with a logistic function using Origin 6.0. For human EAG (Kv10.1) and Kv1.3, peak current inhibition by native BeKm-1 and its analogues was determined during step depolarization from a holding potential of −80 mV to 0 mV or +70 mV, respectively, and normalized to the current recorded without toxin (ITx/ICt).

2.5. Statistical analysis

Data are presented as the mean ± SEM of n oocytes. The statistical significance of the difference between results was determined using the non-paired Student's *t*-test set at the 0.01 level.

3. Results and discussion

3.1. Selection of BeKm-1 residues for branching linkers that bear a fluorescent group

We developed a model using the tetrameric hERG channel structure (PDB 5VA1) to predict BeKm-1 binding mode to the outer part of hERG in order to identify putative solvent-exposed residues on BeKm-1. First, we generated 100 docking models of BeKm-1 in interaction with the outer mouth of the hERG channel using the ZDock and RDock programs (Fig. 1A). Analysis of the top ranked poses from the most populated clusters revealed a predominant orientation of the toxin (Fig. 1B). The proposed binding mode is in good accordance with a previous model generated by Tseng et al. (2007) using the crystal structure of K_vAP pore domain, also in an open conformation, and established from a mutant cycle analysis used to determine the interacting surface between BeKm-1 and the hERG channel (Korolkova et al., 2002). As proposed by Tseng et al., visual inspection of top ranked poses of our study revealed that key residues Lys^{18}, Arg^{20} and Tyr^{11} of BeKm-1 are in contact with the hERG residues Ser^{631}, Gln^{592} and Ile^{583}, respectively, whereas side chain of residues 4, 6, 9, 12, 29, 32, 34 are directed toward the solvent. The side chain of N-terminal Arg^1 and Arg^{27} residues of BeKm-1 were found solvent-exposed in all proposed binding modes and were selected for chemical labeling. Conversely, the C-terminal Phe^{36} residue was more buried in the vast majority of solutions.

3.2. Synthesis of BeKm-1 analogues

On the basis of the information obtained with our model, we synthesized four fluorescent BeKm-1 analogues (Fig. 1B). Three of these analogues took advantage of the solvent accessibility of the most N-terminal residue (Arg^1) of BeKm-1. For these analogues, we extended the N-terminus of the peptide with 4-pentynoic acid (a linker with four additional carbon atoms; linker4), 6-azido-hexanoic acid (a linker with 6 additional carbon atoms; linker6), or 10-undecynoic acid (a linker with 10 additional carbons; linker10). All these linkers are compatible with click chemistry (alkyne function for linker4 and linker10, and

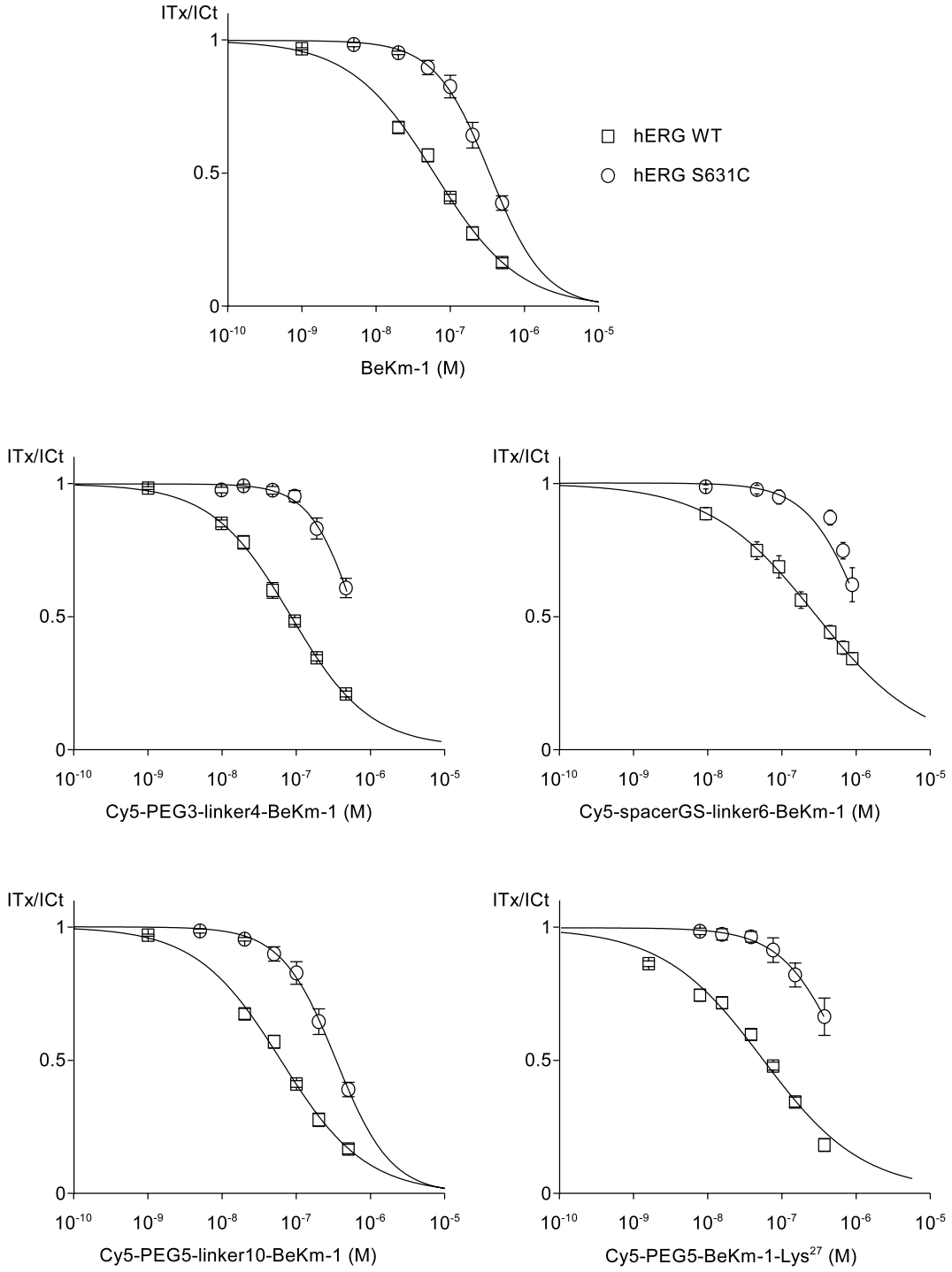

Fig. 4. The mutation S631C in hERG decreases the affinity of native BeKm-1 and of its four fluorescent analogues for the channel. Comparison of the inhibition curves of native BeKm-1 and its four analogues Cy5-PEG3-linker4-BeKm-1, Cy5-spacerGS-linker6-BeKm-1, Cy5-PEG5-linker10-BeKm-1 and Cy5-PEG5-BeKm1-Lys^{27} obtained in *Xenopus laevis* oocytes that express wild type (WT) hERG or the mutant S631C. The data obtained with the mutant channel were fitted by hand for the purpose of comparison. Data are the mean ± SEM of n = 3–5 oocytes.

azide function for linker6). The fourth BeKm-1 analogue was based on the solvent accessibility of Arg^{27}. However, as Arg^{27} is not involved in hERG channel recognition, we replaced this residue by a click chemistry-compatible Lys residue that contains an alkyne function. To all these chemically synthesized click chemistry compatible BeKm-1 analogues, we grafted Cy5-based dyes with additional spacers: Cy5-PEG3-azide to 4-pentynoic-BeKm-1 (**Cy5-PEG3-linker4-BeKm-1**), Cy5-PEG5-azide to 10-undecynoic-BeKm-1 (**Cy5-PEG5-linker10-BeKm-1**), Cy5-spacerGS-Pra to 6-azido-hexanoic-BeKm-1 (**Cy5-spacerGS-linker6-BeKm-1**), and Cy5-PEG5-azide to BeKm-1 Lys(pentynoyl)-OH (**Cy5-PEG5-BeKm-1 Lys^{27}**). Mass spectrometry analyses revealed that the products were correctly synthesized with observed monoisotopic masses of: $[M+5H]^{6+}$ = 809.54 (4852.19 Da *versus* theoretical mass of 4852.72 Da; Cy5-PEG3-linker4-BeKm-1), $[M+5H]^{6+}$ = 838.24 (5024.39 Da *versus* theoretical mass of 5024.37 Da; Cy5-PEG5-linker10-BeKm-1), $[M+4H]^{5+}$ = 1128.31 (5637.51 Da *versus* theoretical mass of 5637.49 Da; Cy5-spacerGS-linker6-BeKm-1) and $[M+5H]^{6+}$ = 819.58 (4912.43 Da *versus* theoretical mass of 4912.27 Da;

Cy5-PEG5-BeKm-1 Lys^{27}) (Supplementary Data S1).

3.3. Effects of native BeKm1 and the four toxin analogues on hERG currents

To investigate the functional consequences of BeKm-1 labeling, we expressed hERG channel in *X. laevis* oocytes. We elicited currents using a classical two-step protocol from a holding potential of −80 mV (Vandenberg et al., 2012). When increasing concentrations of native BeKm-1 were perfused in the bathing solution, the outward current was gradually inhibited (Fig. 2). The IC_{50} value obtained for the native toxin in our recording conditions (12.2 ± 2.2 nM, n = 9) (Table 1) was similar to that obtained in other studies (Hausammann and Grütter, 2013; Zhang et al., 2003). We then performed similar experiments with the four BeKm-1 analogues (Fig. 2). With all of them, we observed a clear dose-dependent inhibition of the outward current, indicating that Cy5 and the linker were grafted at locations that preserved the toxin pharmacophore. However, the IC_{50} values obtained with Cy5-PEG3-linker4-BeKm-1 (88.6 ± 7.6 nM, n = 6), Cy5-PEG5-linker10-BeKm-1 (64.1 ± 6.1 nM, n = 9), Cy5-spacerGS-linker6-BeKm-1 (280.0 ± 41.8 nM, n = 9), and Cy5-PEG5-BeKm-1 Lys^{27} (80.5 ± 10.9 nM, n = 9) were all significantly higher than the IC_{50} value of the native toxin ($p < 0.01$). The least efficient compound was Cy5-spacerGS-linker6-BeKm-1 with a linker that is partly peptidic in nature and highly flexible. This might lead to weak peptide-peptide interactions with BeKm-1 and to a partial neutralization of its activity. This should not occur with the two other analogues in which the linker was attached to the N-terminus, Cy5-PEG3-linker4-BeKm-1 and Cy5-PEG5-linker10-BeKm-1 mainly because their linker is globally shorter. Noteworthy, the Hill coefficient obtained for BeKm-1 and its analogues was close to 1 (Table 1), indicating that the mode of interaction was not altered. Remarkably, with the exception of Cy5-spacerGS-linker6-BeKm-1, our analogues exhibited a lesser affinity than the native toxin but conserved a correct activity with IC_{50}s in the 60–80 nM range.

3.4. Effects of native BeKm-1 and its analogues on the $hK_v10.1$ and $K_v1.3$ currents

We then checked whether labeling affected BeKm-1 specificity or whether the grafted chemical groups induce any block of K^+ channels insensitive to the BeKm-1 toxin. To this aim, we expressed the closely related $hK_v10.1$ (hEAG1) channel and the more distant $hK_v1.3$ channel in *X. laevis* oocytes. We determined the inhibition of the peak outward current measured at 0 mV for hKv10.1 or +70 mV for $hK_v1.3$, from a holding potential of −80 mV, when 200 nM native BeKm-1 or 500 nM toxin analogues were perfused in the bathing solution (Fig. 3). As expected, neither BeKm-1 nor its analogues could inhibit $hK_v10.1$ or $hK_v1.3$ currents at these concentrations (Table 2). We obtained similar results with the *Drosophila melanogaster Shaker* voltage-gated K^+ channel (not shown). We conclude that labelling does not affect BeKm-1 specificity towards hERG and that the grafted chemical groups do not produce unspecific block of these voltage gated K^+ channels.

3.5. Effects of BeKm-1 and its analogues on a mutant hERG channel

Several studies have been devoted to the identification of the residues involved in the inhibition of hERG channel by BeKm-1 (Korolkova et al., 2004, 2002; Tseng et al., 2007). Among the mutation identified in hERG, the S631C mutation decreases BeKm-1 affinity without affecting the channel electrophysiological properties. When exposed to increasing concentrations of native BeKm-1, the hERG mutant channel harboring the S631C mutation was significantly ($p < 0.01$) less inhibited than the wild type hERG channel (IC_{50} = 41 ± 4 nM, n = 5, with mutant hERG vs 12 ± 2 nM, with wild type hERG channel) whereas the Hill coefficient was not changed (0.8 ± 0.1, n = 5, vs 0.9 ± 0.1, n = 9) (Fig. 4). We obtained similar results with the four toxin analogues (Fig. 4 and Table 2). Therefore, we conclude that the four analogues inhibit hERG channel through a similar mechanism than native BeKm-1 toxin.

4. Conclusions

The main goal of this work was to design fluorescent analogues of the hERG-specific BeKm-1 toxin that preserve correct binding to and inhibition of the channel. At the chemical level, the simplest method to covalently attach additional functionalities on peptides or proteins is to make use of the amino-terminal or carboxy-terminal function. In this work, the molecular modeling study illustrates a mode of binding of the toxin where the α-helix (residues S10-F21) is in contact with the hydrophobic surface at the bottom of the binding site of hERG. Because of this preferential orientation of the toxin in its channel-bound configuration and the proximity to the solvent, the N-terminal position of BeKm-1 was selected to attach the PEG3-linker4 and PEG5-linker10 chemical spacers, as well as a Gly/Ser peptide spacer. We also chose the amino acid at position 27 of BeKm-1 to branch a PEG5 chemical spacer on the side chain of a click chemistry-compatible residue localized on the predicted solvent-exposed region of the toxin. In all three PEG spacer-modified toxin cases, the fluorescent analogues exhibited a comparable lower affinity than the native toxin with IC_{50} values in the 60–80 nM range. These findings suggest that Arg^1 and Arg^{27} are probably equivalent in terms of solvent accessibility as proposed on Fig. 1. Also, the length of the chemical spacer did not seem to influence the binding of the toxin to hERG, whereas obviously the Gly/Ser-composed peptide spacer leads to a more drastic 23-fold decrease in activity. This observed difference may be due to interactions between the toxin and the peptide spacer that alter the BeKm-1 pharmacophore to some extent. As reported by Wang and MacKinnon (2017), the hERG channel is relatively instable when solubilized in detergent. Considering their very acceptable affinities of less than 100 nM, the three fluorescent Bekm-1 analogues could be useful tools to follow and discriminate functional tetrameric hERG during the biochemical purification of the channel. On the other hand, it is worth noting that reports of membrane receptors or channel visualization at the cellular level with fluorescent toxins mostly made use of molecular probes showing nanomolar or even better affinities (Kuzmenkov et al., 2016; Schembri et al., 2015). Further studies using other residues of Bekm-1 such as K6 or D34 which are predicted to be solvent-exposed, could provide analogues with even better affinities than those described in this report. Ongoing chemical syntheses will allow testing this hypothesis in the near future. Results obtained in this study suggest that protein-protein docking tools greatly facilitate the design of modified toxins that may be used as reporters in ion channel imaging or in biochemical purification/characterization efforts. In association with the Ala-scan investigations of the expected solvent exposed residues, to better define which terminal group or side chain to be grafted, a similar approach could be envisaged for producing fluorescent analogues for a large numbers of toxins. Finally, it is noteworthy that the chemistry used in our work remained compatible with the proper folding of Bekm-1 and will be routinely extended to new toxins or new amino acid positions to be grafted in Bekm-1.

Conflict of interest

The authors declare that they have no conflicts of interest concerning the contents of this article.

Acknowledgements

This work was supported by CNRS, Inserm, Université de Montpellier. MDW thanks the Fondation Leducq and FEDER for financial support. MDW acknowledges the financial support from the Agence Nationale de la Recherche to the LabEx Ion Channels, Science and Therapeutics (ANR-11-LABX-0015). The authors wish to express

their deep grateful to Dr Maguy DEL-RIO for her help during this work.

Transparency document

Transparency document related to this article can be found online at https://doi.org/10.1016/j.toxcx.2019.100010

Appendix A. Supplementary data

Supplementary data to this article can be found online at https://doi.org/10.1016/j.toxcx.2019.100010.

References

Angelo, K., Korolkova, Y.V., Grunnet, M., Grishin, E.V., Pluzhnikov, K.A., Klaerke, D.A., Knaus, H.-G., Müller, M., Olesen, S.-P., 2003. A radiolabeled peptide ligand of the hERG channel, [125 I]-BeKm-1. Pflügers Arch. Eur. J. Physiol. 447, 55–63. https://doi.org/10.1007/s00424-003-1125-9.

Beeton, C., Wulff, H., Standifer, N.E., Azam, P., Mullen, K.M., Pennington, M.W., Kolski-Andreaco, A., Wei, E., Grino, A., Counts, D.R., Wang, P.H., LeeHealey, C.J., Andrews, B.S., Sankaranarayanan, A., Homerick, D., Roeck, W.W., Tehranzadeh, J., Stanhope, K.L., Zimin, P., Havel, P.J., Griffey, S., Knaus, H.-G., Nepom, G.T., Gutman, G.A., Calabresi, P.A., Chandy, K.G., 2006. Kv1.3 channels are a therapeutic target for T cell-mediated autoimmune diseases. Proc. Natl. Acad. Sci. U. S. A. 103 17414–9. https://doi.org/10.1073/pnas.0605136103.

Bergeron, Z.L., Bingham, J.-P., 2012. Scorpion toxins specific for potassium (K+) channels: a historical overview of peptide bioengineering. Toxins (Basel) 4, 1082–1119. https://doi.org/10.3390/toxins4111082.

Boutin, J.A., Li, Z., Vuillard, L., Vénien-Bryan, C., 2016. Cryo-microscopy, an alternative to the X-ray crystallography? Med. Sci. (Paris) 32, 758–767. https://doi.org/10.1051/medsci/20163208025.

Chandy, K.G., Norton, R.S., 2017. Peptide blockers of K v 1.3 channels in T cells as therapeutics for autoimmune disease. Curr. Opin. Chem. Biol. 38, 97–107. https://doi.org/10.1016/j.cbpa.2017.02.015.

Chiu, P.J.S., Marcoe, K.F., Bounds, S.E., Lin, C.-H., Feng, J.-J., Lin, A., Cheng, F.-C., Crumb, W.J., Mitchell, R., 2004. Validation of a [3H]astemizole binding assay in HEK293 cells expressing HERG K+ channels. J. Pharmacol. Sci. 95, 311–319.

de Souza, J.M., Goncalves, B.D.C., Gomez, M.V., Vieira, L.B., Ribeiro, F.M., 2018. Animal toxins as therapeutic tools to treat neurodegenerative diseases. Front. Pharmacol. 9, 145. https://doi.org/10.3389/fphar.2018.00145.

Finlayson, K., Turnbull, L., January, C.T., Sharkey, J., Kelly, J.S., 2001. [3H]dofetilide binding to HERG transfected membranes: a potential high throughput preclinical screen. Eur. J. Pharmacol. 430, 147–148.

Hancox, J.C., McPate, M.J., El Harchi, A., Zhang, Y. hong, 2008. The hERG potassium channel and hERG screening for drug-induced torsades de pointes. Pharmacol. Ther. 119, 118–132. https://doi.org/10.1016/j.pharmthera.2008.05.009.

Hausammann, G.J., Grütter, M.G., 2013. Chimeric hERG channels containing a tetramerization domain are functional and stable. Biochemistry 52, 9237–9245. https://doi.org/10.1021/bi401100a.

Housley, D.M., Housley, G.D., Liddell, M.J., Jennings, E.A., 2017. Scorpion toxin peptide action at the ion channel subunit level. Neuropharmacology 127, 46–78. https://doi.org/10.1016/J.NEUROPHARM.2016.10.004.

Korolkova, Y.V., Bocharov, E.V., Angelo, K., Maslennikov, I.V., Grinenko, O.V., Lipkin, A.V., Nosyreva, E.D., Pluzhnikov, K.A., Olesen, S.-P., Arseniev, A.S., Grishin, E.V., 2002. New binding site on common molecular scaffold provides HERG channel specificity of scorpion toxin BeKm-1. J. Biol. Chem. 277, 43104–43109. https://doi.org/10.1074/jbc.M204083200.

Korolkova, Y.V., Kozlov, S.A., Lipkin, A.V., Pluzhnikov, K.A., Hadley, J.K., Filippov, A.K., Brown, D.A., Angelo, K., Strøbaek, D., Jespersen, T., Olesen, S.P., Jensen, B.S., Grishin, E.V., 2001. An ERG channel inhibitor from the scorpion Buthus eupeus. J. Biol. Chem. 276, 9868–9876. https://doi.org/10.1074/jbc.M005973200.

Korolkova, Y.V., Tseng, G.-N., Grishin, E.V., 2004. Unique interaction of scorpion toxins with the hERG channel. J. Mol. Recogn. 17, 209–217. https://doi.org/10.1002/jmr.667.

Kuzmenkov, A.I., Nekrasova, O.V., Kudryashova, K.S., Peigneur, S., Tytgat, J., Stepanov, A.V., Kirpichnikov, M.P., Grishin, E.V., Feofanov, A.V., Vassilevski, A.A., 2016. Fluorescent protein-scorpion toxin chimera is a convenient molecular tool for studies of potassium channels. Sci. Rep. 6, 33314. https://doi.org/10.1038/srep33314.

Lastraioli, E., Lottini, T., Bencini, L., Bernini, M., Arcangeli, A., 2015. hERG1 potassium channels: Novel biomarkers in human solid cancers. BioMed Res. Int. 2015, 1–9. https://doi.org/10.1155/2015/896432.

Milnes, J.T., Dempsey, C.E., Ridley, J.M., Crociani, O., Arcangeli, A., Hancox, J.C., Witchel, H.J., 2003. Preferential closed channel blockade of HERG potassium currents by chemically synthesised BeKm-1 scorpion toxin. FEBS Lett. 547, 20–26. https://doi.org/10.1016/S0014-5793(03)00662-8.

Schembri, L.S., Stoddart, L.A., Briddon, S.J., Kellam, B., Canals, M., Graham, B., Scammells, P.J., 2015. Synthesis, biological evaluation, and utility of fluorescent ligands targeting the μ-opioid receptor. J. Med. Chem. 58, 9754–9767. https://doi.org/10.1021/acs.jmedchem.5b01664.

Tarcha, E.J., Olsen, C.M., Probst, P., Peckham, D., Muñoz-Elías, E.J., Kruger, J.G., Iadonato, S.P., 2017. Safety and pharmacodynamics of dalazatide, a Kv1.3 channel inhibitor, in the treatment of plaque psoriasis: A randomized phase 1b trial. PLoS One 12, e0180762. https://doi.org/10.1371/journal.pone.0180762.

Tseng, G.-N., Sonawane, K.D., Korolkova, Y.V., Zhang, M., Liu, J., Grishin, E.V., Guy, H.R., 2007. Probing the outer mouth structure of the HERG channel with peptide toxin footprinting and molecular modeling. Biophys. J. 92, 3524–3540. https://doi.org/10.1529/biophysj.106.097360.

Uysal, S., Vasquez, V., Tereshko, V., Esaki, K., Fellouse, F.A., Sidhu, S.S., Koide, S., Perozo, E., Kossiakoff, A., 2009. Crystal structure of full-length KcsA in its closed conformation. Proc. Natl. Acad. Sci. 106, 6644–6649. https://doi.org/10.1073/pnas.0810663106.

Vandenberg, J.I., Perry, M.D., Perrin, M.J., Mann, S.A., Ke, Y., Hill, A.P., 2012. hERG K(+) channels: structure, function, and clinical significance. Physiol. Rev. 92, 1393–1478.

Wang, W., MacKinnon, R., 2017. Cryo-EM Structure of the Open Human Ether-à-go-go-Related K + Channel hERG. Cell 169, 422–430. e10. https://doi.org/10.1016/j.cell.2017.03.048.

Whicher, J.R., MacKinnon, R., 2016. Structure of the voltage-gated K^+ channel Eag 1 reveals an alternative voltage sensing mechanism. Science 353, 664–669. https://doi.org/10.1126/science.aaf8070.

Zhang, M., Korolkova, Y.V., Liu, J., Jiang, M., Grishin, E.V., Tseng, G.-N., 2003. BeKm-1 Is a HERG-Specific Toxin that Shares the Structure with ChTx but the Mechanism of Action with ErgTx1. Biophys. J. 84, 3022–3036. https://doi.org/10.1016/S0006-3495(03)70028-9.